Combustion of Single Biomass Particles in Air and in Oxy-Fuel Conditions

Juan Riaza[1], Reza Khatami[2], Yiannis A. Levendis[2*], Lucia Álvarez[1], Maria V. Gil[1], Covadonga Pevida[1], Fernando Rubiera[1], Jose J. Pis[1]

[1] Instituto Nacional del Carbón, INCAR-CSIC, Apartado 73, 33080 Oviedo, Spain

[2] Mechanical and Industrial Engineering Department, Northeastern University, Boston, MA, 02115, USA

* Corresponding author: y.levendis@neu.edu

Tel: 1 (617) 373-3806, Fax: 1 (617) 373-2921

Abstract

The combustion behaviors of four different pulverized biomasses were evaluated in the laboratory. Single particles of sugar cane bagasse, pine sawdust, torrefied pine sawdust and olive residue were burned in a drop-tube furnace, set at 1400 K, in both air and O_2/CO_2 atmospheres containing 21, 30, 35, and 50% oxygen mole fractions. High-speed and high- resolution images of single particles were recorded cinematographically and temperature-time histories were obtained pyrometrically. Combustion of these particles took place in two phases. Initially, volatiles evolved and burned in spherical envelope flames of low luminosity; then, upon extinction of these flames, char residues ignited and burned in brief periods of time. This behavior was shared by all four biomasses of this study, and only small differences among them were evident based on their origin, type and pre-treatment. Volatile flames of biomass particles were much less sooty than those of previously burned coal particles of analogous size and char combustion durations were briefer. Replacing the background N_2 gas with CO_2, i.e., changing from air to an oxy-fuel atmosphere, at 21% O_2 impaired the intensity of combustion; reduced

the combustion temperatures and lengthened the burnout times of the biomass particles. Increasing the oxygen mole fraction in CO_2 to 28-35% restored the combustion intensity of the single biomass particles to that in air.

Keywords: biomass process residues; torrefied biomass; combustion; ignition; single particle; pyrometry.

1. Introduction

Biomass has higher volatile matter content than coal, but it has less carbon, more oxygen and a lower energy content (heating value). The use of biomass in existing pulverized coal power plants requires only minor modifications as compared to the construction of new biomass-specific fired power plants, making the co-firing of biomass with coal an easier and less costly way for generating power. Co-firing is becoming more common in coal power plants because replacing part of the coal with biomass results in lower pollutant and greenhouse gas emissions, as compared to firing neat coal [1, 2]. Co-firing biomass and coal reduces the emissions of SO_2, NO_x and CO_2. Altogether elimination of such emissions may be achieved in future power plants (termed zero emission power plants) by implementing carbon dioxide capture and storage (CCS) techniques. However, co-firing coal with biomass reduces the power output of a power-plant in proportion to the amount of the latter fuel [3, 4, 5].

Oxy-fuel combustion is a promising technology for facilitating CCS. It burns fuel in a mixture of oxygen and recycled flue gases (mainly CO_2) instead of air in conventional combustion. The exhaust flue gases consist mainly of CO_2, approx. 95% on a dry volume basis, and small amounts of excess oxygen, nitrogen and, to a lesser extent,

pollutants, such as nitrogen oxides (NO_x) and sulfur oxides (SO_x) (approx. 0.1– 0.2% dry volume basis) [6]. The combination of oxy-fuel combustion, as a CCS technology, with biomass [2] could effectively provide a method which would not only avoid further CO_2 emissions but, perhaps even help reduce the atmospheric CO_2. Simpson et al. [7] compared the efficiency of oxy-fuel combustion and post-combustion carbon dioxide separation cycles by thermodynamic analysis. They concluded that the air separation efficiency in oxy-fuel technology must increase sufficiently to offset the additional cost and inefficiency of requiring a CO_2 purification unit on the back end. They proposed that oxy-fuel combustion may be more attractive for systems operating with oxygenated fuels such as biomass. For such systems, the development of near-stoichiometric combustors would not need expensive CO_2 purification units. Moreover, a recent investigation [8] revealed that biomass/coal blend combustion may be a method for controlling the excess heat generated from oxy-combustion of coal, a proposed "clean" coal technology. They utilized a TGA-DSC technique at 1173 K to burn blends of a lignite coal and two biomasses, at high oxygen partial pressures. They reported that the heat flux from the combustion of lignite increased dramatically when the oxidizing medium was altered from dry air to neat oxygen. However, in the case of co-firing lignite with biomass under neat oxygen, the excess heat flux arising from the combustion of lignite was reduced and the temperature of the combustion chamber was thus controlled. Based on their results, they suggested that co-combustion of coal/biomass blends in enriched oxygen environments may be an alternative method to CO_2 recycling in future oxy-fuel combustion systems.

All biomasses are composed of three main components: cellulose, hemicellulose and lignin. For instance, the sugar-cane bagasse sample burned herein contained 41.3%

cellulose, 34.3% hemicelluloses and 13.8% lignin. Whereas cellulose and hemicellulose are macromolecules constructed from different sugars, lignin is an aromatic polymer synthesized from phenylpropanoid precursors [9]. Hemicellulose is easily degraded, and its pyrolysis takes place at temperatures in the range of 493–588 K. The pyrolysis of cellulose occurs in the 588–673 K range, whereas that of lignin covers a wider temperature range (423–1176 K) [10].

Torrefaction is a useful pre-treatment for the biomass materials as they are sometimes difficult to fluidize and introduce into furnaces because of their fibrous shapes [11]. The management and milling of torrefied biomass is easier than that of the parent biomass. That is why the torrefaction process is being introduced to industrial practices [12, 13]. This process consists of heating the biomass in nitrogen, or in a low oxygen-containing atmosphere, to temperatures up to 573 K. In this process, the biomass dries, and as the temperature increases, certain changes take place in the molecular structure. Light hydrocarbon molecules are released through the decomposition of the reactive hemicellulose fraction [14]. Torrefied fuels are easier to manage, and they contain more fragile particles as well as a higher energy density than the parent biomass particles [15, 16]. During the torrefaction process, the biomass loses typically 30% of its mass, but only 10% of its energy content [17]. The resulting higher energy density of the torrefied fuel reduces the transportation costs.

Biomass pyrolysis has been investigated in numerous studies. Results are highlighted in several reviews, including those in Refs. [3, 18, 19, 20, 21, 22]. The pyrolytic products are H_2, H_2O, CO, CO_2, CH_4, other light hydrocarbons, tar, ash and char. At temperatures below 773 K, biomass fuels decompose into primary volatiles. At these temperatures, tars are produced by depolymerisation reactions while pyrolytic water is produced by

dehydration reactions. The main gaseous products of pyrolysis are CO_2 and CO. At temperatures above 773 K, the primary volatiles are subject to a secondary pyrolysis, during which tars are converted into a variety of gaseous species, especially CO, light hydrocarbons, hydrogen and CO_2. At high heating rates, biomass decomposes expediently generating mostly gas, vapors and char [23]. The char that remains upon termination of the pyrolysis reactions is enriched in carbon [24].

Implementation of optical pyrometry and high speed cinematography for the study of ignition and combustion of single coal particles and streams of coal particles has been well documented [25, 26, 27, 28, 29, 30, 31, 32, 33]. However, there is a scarcity of analogous studies on biomass particle ignition and combustion characteristics. On the other hand, Wornat et al. [34] studied the combustion rates of single particles of two biomass chars (southern pine and switch grass), with nominal sizes in the range of 75-106 μm, in a laminar flow reactor with 6% and 12% O_2 mole fraction (balance N_2) at 1600 K. In situ measurements using a two-color optical pyrometer and a video camera revealed that biomass char particles burned over a wider temperature range (1500-1950K, $\Delta T \approx 450$ K) than high volatile bituminous and lignite coal particles (1800-1950K , i.e., $\Delta T \approx 150$ K versus 1900-2000 K, i.e., $\Delta T \approx 100$ K, respectively). Austin et al. [35] conducted an experimental study in a drop-tube furnace, burning 300-1500 μm corncob particles in air using a video camera (50-100 frames per second) and an infrared phototransistor. They determined that the burning times of the volatiles and the ignition delay times increased with the increase of the initial particle density and diameter. Meesri and Moghtaderi [36] burned pine sawdust particles at drop-tube furnace temperatures of 1473K in air and reported particle temperatures circa 1700K. They also reported that the char oxidation reactions occurred in Regime II, where

chemical reactions and pore diffusion happen concurrently. Arias et al. [37] studied the ignition and combustion characteristics of coal/biomass blends under oxy-fuel conditions. They burned a bituminous coal and bituminous coal/eucalyptus biomass blends (90%-10% or 80%-20%, by weight) Their experiments were performed in an electrically-heated entrained flow reactor (EFR) set to 1273 K. Oxy-fuel combustion of pulverized fuels (75-150 μm) occurred with 21%, 30% and 35% O_2 mole fraction in CO_2, and was compared with results obtained in air. When coal was blended with the biomass, its ignition temperature in air was reduced. However, this effect was less pronounced in the case of oxy-fuel combustion, regardless of O_2 concentration. The effect of blending biomass and coal on burnout effectiveness was negligible. Riaza et al. [2] observed similar results. Borrego et al. [38] obtained chars from different biomasses by pyrolysis in air and in oxy-fuel environments, and reported no significant differences between the char characteristics, i.e., pore volume, morphology, surface area and reactivity.

In addition to the above studies, some other notable investigations reported on experiments and numerical modeling of single-particle biomass combustion [39, 40, 41, 42]; however, the number of experimental works on this topic is very limited [43]. Additional studies are warranted to document the entire combustion behavior of biomass fuels, especially the phase of the volatile matter combustion. Such studies may be instrumental in assessing the radiating behavior of biomass particles in furnaces. In particular, little (if anything) has been reported on the experimental combustion behavior of individual biomass particles in oxy-combustion conditions, and this is of special interest to co-firing coal and biomass in future oxy-fuel power plants. The present work reports on systematic *in situ* combustion study of different biomasses

(residual or torrefied) in a laboratory-scale drop-tube furnace, under both conventional (air) and oxy-fuel conditions by means of optical pyrometry and high-speed back-light cinematography. Comparisons with the combustion characteristics of coal particles studied in previous work in this laboratory are made.

2. Bio-Fuel Characteristics and Experimental Methods

2.1. Biomass samples

Four different residue biomasses were studied, olive residue (OR), which are residues from the olive oil production industry, pine sawdust (PI), torrefied pine sawdust (TOPI), and sugarcane bagasse (SCB), which is a residue of bio-ethanol and sugar production. Olive residue is the part of the olive that remains after the olive oil has been extracted. Nowadays olive residue biomass is used as a low cost renewable fuel for domestic and industrial heating. The olive residue sample used in this work was supplied by ELCOGAS, S.A., which is an IGCC power station located in Puertollano (Ciudad Real, Spain), that processes a 50:50 blend (based on weight) of coal and petcoke, and occasionally also includes biomass in the fuel blend. The pine sawdust sample was obtained from a pellets industry, Pellets Asturias, S.L., situated in Tineo (Asturias, Spain), which has a yearly production of 30,000 tons of pellets. The torrefaction of pine sawdust was carried out at INCAR-CSIC. The torrefaction treatment conditions were selected according to the results obtained in previous studies [15]. Briefly, the torrefaction of pine sawdust was performed using a horizontal quartz reactor, where 10–15 g of biomass was heated at a rate of 10 K min^{-1} under a nitrogen flow rate of 50 mL min^{-1} up to 513 K. The samples were kept at the final temperature for 1 hour. The mass loss from the sample was measured and then the sample was sieved to 75-150 μm.

Sugar cane bagasse was collected directly from a mill located in Brazil – São Paulo State. The bagasse was washed, dried at 90°C for 24 hours, chopped in a household blender and sieved. All biomass samples were less than a year old and were kept in closed glass bottles in the laboratory under standard temperature and pressure conditions.

Photographs and scanning electronic microscope images of the different biomasses samples are presented in Fig. 1. All of the samples were ground and sieved to 75-150 μm. The proximate and ultimate analyses and gross calorific values of the biomasses are given in Table 1.

2.2. Experimental Approach

2.2.1. Drop-tube furnace (DTF)

An electrically-heated laminar-flow drop-tube furnace was used for the combustion experiments. The furnace (an *ATS* unit) was fitted with an alumina tube (*Coors*) with an inner diameter of 7 cm. It was heated with molybdenum disilicide heating elements, defining a radiation zone of 25 cm in length. The furnace was fitted at the top with a water-cooled injector (Fig. 2a). Details of the design of the furnace injector are provided elsewhere [30, 44]. To introduce single biomass particles into the furnace injector, the following technique was used. A few particles were placed inside the tip of a beveled syringe needle. The needle was inserted into a port at the top of the injector, which was rotated half a revolution back and forth and then gently tapped. Single particles could thus be dropped into the furnace injector. Upon exiting the injector, the particles reacted with the preheated furnace gases. The furnace wall temperatures (T_f) were continuously monitored by type-S thermocouples embedded in the wall. Particle heating rates were

very high, calculated to be in the order of 10^4 K s^{-1}. Optical access to the radiation zone of the furnace was achieved through three observation ports: one at the top (Pyrometer) and two orthogonally situated at the sides of the furnace. The pyrometer and the high speed cinematography camera were used as experimental devices to study the burning of single biomass particles.

2.2.2. Optical pyrometer

Pyrometric observations of burning single particles were conducted from the top of the furnace injector, viewing downward along the central axis of the furnace is typically a particle's path-line. Thus, complete luminous burnout histories of single biomass particle - from ignition to extinction - were monitored. An optical fiber made up of a high- transmittance (> 99.5%) fused silica core and doped fused silica cladding with an *f*-number of 2.2, transmitted light from the furnace to the pyrometer assembly. The pyrometer used two dichroic edge filters as spectrum splitters to direct the light to the three interference filters (Fig.2b). These filters had effective wavelengths of 0.640, 0.810 and 0.998 μm with bandwidths (FWHM) of 70 nm. In conjunction with these interference filters, silicon diode detectors were employed to maximize the signal sensitivity. They also possessed good stability and linearity. Details of the pyrometer optics and electronics were supplied by Levendis et al. [28, 30]. The voltage signals generated by the three detectors were amplified and then processed by a microcomputer using *LabView* software. The temperature was deduced from the three output voltage signals of the pyrometer using a non-linear least square method, based on Planck's radiation law. Details of this method were supplied by Khatami and Levendis [44].

2.2.3. High-speed camera

High-speed cinematography was conducted through the slotted side quartz windows of the drop-tube furnace against backlight (Fig. 2a). A *NAC HotShot 512SC* self-contained digital high-speed video camera was used, at speeds of 1000 or 2000 frames/s. The camera was fitted with an *Infinity* model K2 long-distance microscope lens to provide high-magnification images of the combustion events (Fig.2c).

2.3. Gas temperatures and Furnace Gas Compositions

Combustion experiments of biomass particles were conducted under a quiescent gas condition (i.e., no gas flow). Quiescent gas condition was created by turning off the gas flows 10 seconds prior to the particle injection. The design of this experiment has been documented by Khatami et al. [33]. A slender bare thermocouple (*Omega* type K) was used to measure the axial profile of the centerline gas temperature. The measured temperatures with this method were corrected for radiation effects as outlined by Khatami et al. [33]; results are illustrated in Fig.3. Under the quiescent gas condition (no flow), the gas temperature profiles were similar in either N_2 or CO_2 environments. Both temperatures increased along the centerline of the furnace and stabilized at an estimated 1340 K. The furnace wall set-point temperature (T_w) was 1400 K, as monitored by type-*S* thermocouples embedded in the wall. The gas compositions in the furnace included air as well as mixtures of oxygen (mole fractions of 21 $\%O_2$, 30$\%O_2$, 35$\%O_2$ and 50$\%O_2$) in carbon dioxide to simulate oxy-combustion conditions. In this manuscript all gas compositions are given on a mole fraction basis, which is equivalent to a volume fraction basis, as percentages (%).

3. Results and Discussion

3.1. Cinematographic observations

Six snapshot photographic sequences for each biomass sample at different gas atmospheres during burnout history of the particle are shown in Fig. 4. The particles ignited very close to the injector tip at the top of the DTF, immediately upon entering the radiation zone. Upon ignition, the flames surrounding individual particles grew bigger and increasingly luminous. For all biomass fuels at all gas compositions, the envelope flames had strikingly spherical shapes with fairly uniform luminosity. Some other similar burning characteristics were also observed for all the biomasses. The similarities included the sequential particle devolatilization with ignition and burning of the volatiles around the particle, followed by the ignition, combustion and extinction of the char residues.

The ignition of particles was determined visually as the onset of luminous combustion. However, the determination of the precise initial instant of ignition of the volatile matter proved to be difficult for several reasons. Firstly, as Grotkjaer et al. [45] have already pointed out, the ignition temperatures of biomass are fairly low and lie in the range of 500-600 K in air. In this study, the volatiles ignition took place at temperatures much lower than the furnace wall temperature (1400 K) and could not be categorically discerned by optical techniques. Secondly, the volatiles envelope flames had low luminosities and typically exhibited low contrast with the background furnace surfaces.

3.2. Pyrometric Signals

Figure 5 shows sample radiation intensity signals, corresponding to the 0.640, 0.810 and 0.998 μm pyrometric wavelengths, obtained from single particles of each type of

biomass burning in air. As can be seen in this figure, the signals of the PI, TOPI and SCB particles exhibit two different zones: the first peak corresponds to volatiles combustion in envelope flames and the second peak corresponds to subsequent char combustion. The first peak (corresponding to volatiles combustion) of OR signals is much weaker than that of other biomass samples.

3.3. Combustion temperatures and burnout times

To facilitate a quantitative comparison between the different biomass fuels burning in the diverse atmospheres of this study, burnout times of the volatiles and burnout times of chars were directly obtained from both pyrometric and cinematographic observations, whereas char combustion temperatures were deduced from pyrometric data. The particle burnout times, displayed in Figs. 6 and 7, were deduced from pyrometric signals for volatile matter and char combustion phases, based on the duration of the recorded highest-intensity signal (λ = 0.998 μm) of a particular event from its onset (particle ignition) to its termination (particle extinction), both defined when the signal exceeded its baseline by a factor of at least one thousand, i.e., $S_{signal}/S_{baseline} > 1{,}000$. Each data point represents mean values from a minimum of 15 individual particle combustion events. Standard deviation bars (2σ) are shown on each datum point. Volatile burnout times recorded by cinematography (e.g., see Fig.4) were typically shorter (by 10%) than the pyrometric volatile burnout times (Fig. 6). The discrepancy between pyrometric and cinematographic volatile burnout times was attributed to the fact that low-luminosity, nearly-transparent flames are hard to identify visually in photographic records (visible bandwidth is 0.4-0.7 μm), whereas the pyrometer is able to record radiation emanating from non-sooty flames at the near-infrared wavelengths of 0.81 μm and 0.998 μm. In

the case of the olive residue biomass (OR) which have lower volatile matter content than the other biomasses, the duration of the volatile matter combustion phase could not be reliably assessed because even the pyrometric signals were too weak. However, the volatiles combustion peaks were clearly distinguishable in the cases of SCB, PI and TOPI biomasses (see Fig. 5).

The volatile matter flame temperature deduction method is currently under development in this laboratory for such lowly-sooty flames, for which the gray-body emissivity assumption [44] may not be valid. Thus, the temperatures of the volatile matter flames are not reported herein. The presented char temperatures in Fig. 8 are peak temperatures recorded in individual particle burnout histories, averaged over at least 15 single particle cases. Char temperatures were deduced by the method of Khatami and Levendis [44].

3.4 Effect of atmospheric composition (replacement of N_2 by CO_2) and O_2 mole fraction

3.4.1. Combustion Behavior

The weakest particle combustion intensities were obtained in the 21%O_2-79%CO_2 atmosphere for all biomass samples. The weaker particle combustion intensities in 21%O_2-79%CO_2 atmosphere than in air are due to the lower particle temperatures, which resulted from the lower diffusivity of oxygen in CO_2 than in N_2 [46, 47]. It has also been determined that the higher volumetric heat capacity of CO_2 (than N_2) contributes to the lower particle temperatures [47].

At 21% O_2, both in the N_2 and CO_2 environments, the ignition and combustion of the volatiles and the ignition of the char residues occurred sequentially in a particle's time-history profile (Fig. 4). When the combustion of the volatiles was completed, the flame

extinguished and, subsequently, char ignition took place. Some differences were observed in the time periods between volatile extinction and char ignition in air and in the 21%O_2/79%CO_2 atmosphere; the former was in the neighborhood of 2 ms, whereas the latter was much lengthier, at 5-8 ms.

At higher oxygen mole fractions (>30%) in CO_2, the following behaviors were observed: (i) ignition of the volatiles started earlier, i.e., the ignition delay period was briefer; (ii) the volatile flames were less bright (e.g., see Fig. 4: bagasse at 35% and 50% O_2 mole fractions), most likely because under such conditions soot oxidation reactions were more prominent than soot formation reactions in the envelope flames; and finally, (iii) the incandescent residual char particles of all fuels emitted stronger radiation and they appeared brighter. In the 50%O_2-50%CO_2 atmosphere, chars ignited while the volatiles were still burning. At such an elevated oxygen mole fraction, the phases of the homogeneous volatiles combustion and heterogeneous residual char combustion became nearly indistinguishable. Moreover, char combustion was very fast.

3.4.2. Temperatures and burnout times

Devolatilization of particles occurs both pre- and post-ignition in the furnace. Pre-ignition devolatilization times are affected by the ignition delay period, which is in turn influenced by the volumetric heat capacity (heat sink) of the surrounding gas. Post-ignition devolatilization times are affected by the flame temperature, which is influenced by the composition, and thus, the properties of the surrounding gas. Hence, both times are affected by the substitution of N_2 with CO_2 gas in oxy-combustion. In this work, only the post-ignition devolatilization and simultaneous volatiles combustion phenomena could be monitored. In general, longer volatile and char burnout times were

observed when N_2 was replaced by CO_2, at the same oxygen mole fraction (i.e., longer burnout times in 21%O_2/79%CO_2 than in 21%O_2/79%N_2), see Figs 6 and 7. Moreover, the burnout time decreased as the oxygen mole fraction increased from 21% to 35%. These results are in agreement with previous studies which were carried out for coal particles of all ranks [2, 32, 48]. In the cases of both coal and biomass char particles it is likely that combustion occurred in Regime II, i.e., under both kinetic and diffusion control [44]. For biomass chars this was illustrated with calculations outlined in the Appendix, whereas for coal chars, burning under identical conditions, similar calculations have been performed in Refs. [32] and [48]. Figure 7 shows that increasing the O_2 mole fraction further, from 35% to 50%, had a less pronounced effect on the char burnout time. Peak char temperatures, averaged over particles, during combustion of biomass in both air and simulated oxy-fuel conditions, shown in Fig. 8, are heavily dependent on the oxygen mole fraction. The temperatures of all biomass particles burning in air were higher than those burning in 21%O_2 diluted with CO_2. At higher oxygen mole fractions (>21%) in CO_2, the char combustion temperatures increased while the durations of char combustion decreased. Increasing the oxygen mole fraction in CO_2 to 30-35% restored the combustion intensity of single fuel particles to the level found in conventional combustion in air, for all biomass fuels tested herein. This is in agreement with observations on coal particle combustion reported in Ref. [33].

3.5. Effect of biomass type

Biomass particles burned expediently under the conditions of this work. Biomass devolatilization commences at low temperatures (at around 473 K [19, 45]). As the particles heated up, devolatilization accelerated until most of the volatiles were released.

The heating rate of the particles in the drop tube furnace was high (in the order of 10^4 K s^{-1} [34]). Biomass structures, and heavy hydrocarbons and tars, produced by the devolatilization step have been reported to expediently convert into smaller molecules by cracking reactions in the proximity of the devolatilizing particles [49]. In fact, previous work in this laboratory [50, 51, 52, 53] pyrolyzed various biomasses under relevant high heating-rate conditions and elevated furnace temperatures and found that the pyrolytic products were mainly light hydrocarbon gases (such as methane, ethylene, ethane, acetylene, propylene, benzene, ethyl-benzene, etc.), as well as hydrogen, carbon monoxide and carbon dioxide.

The proximate and ultimate analyses of the different biomasses were similar, see Table 1, and so was their combustion behavior. The sugarcane bagasse, SCB, has the highest volatile matter content, therefore extra time was likely needed for devolatilization, and the combustion duration of the volatiles of this fuel was indeed observed to be lengthier (see Fig. 6). On the other hand, SCB has the least fixed carbon content and, thus, it exhibited the shortest char burnout duration (Fig. 7).

The envelope flames of olive residues, OR, were slightly less distinguishable cinematographically than those of the other biomass fuels. The corresponding pyrometric signals were also weaker than those of the rest of the samples. It is notable that OR had the lowest volatile matter content than the rest of the biomasses examined herein. Moreover, it was found that the OR char temperatures were the lowest among those of the other fuels, in all gas atmospheres in the DTF and the burnout times of the OR chars were less influenced by the oxygen mole fraction in the gas, as shown in Fig. 7. Regarding the combustion behavior of the chars, it is notable that OR had the highest ash, which may have increased the catalytic effect on the char burnout and have thus

decreased the influence of oxygen content of the surrounding gas. High ash content and possible, yet unexplored, physical structure-related reasons (pore sizes, porosity, tortuosity) may have been responsible for the lower char temperatures.

The torrefied pine sawdust (TOPI) chars burned hotter than the other biomass chars under all oxy-fuel conditions. Differences in the combustion behavior of the pine sawdust (PI) and the torrefied pine sawdust (TOPI) were very small. However, a more luminous flame was observed in the case of TOPI (Fig. 4). This is perhaps because a lower amount of CO_2 was supposedly released with the TOPI volatiles as a consequence of the torrefaction pre-treatment while the hydrogen content of the torrefied sample and, therefore, the release of hydrocarbon gases (e.g. CH_4 and C_2H_6) remained unchanged [15]. The CO_2 dilutes the rest of the combustible gases and produces lower luminosity flames. The TOPI biomass released a greater amount of energy per unit mass during combustion due to the fact that its calorific value was higher than that of raw biomass (PI). This effect was confirmed by the typically hotter char temperatures of TOPI. Average volatile burnout times of the original PI were longer; however, the char combustion times were generally similar, perhaps a little shorter for the original PI in comparison with the torrefied TOPI under oxy-fuel atmospheres.

3.6 On the differences of single-biomass and single-coal particle combustion

Several recent studies in this laboratory have focused on the combustion behavior of coal particles of all ranks in conventional (air) and oxy-fuel conditions [30, 31, 32, 48]. In comparison to coal, biomass particles exhibit certain physical and chemical differences, the most prominent of which have as follows: (1) Raw biomasses have a highly fibrous nature. (2) The biomass particles are less dense than coal particles,

therefore the total mass burnt for the same nominal particle size is lower. (3) Biomass has much lower heating value than coals [20], see also Tables 1 and Table A2 in Appendix 2. (4) Biomass has a different elemental composition with a high proportion of oxygen. See Tables 1 and Table A2 in Appendix 2. (5) The proximate composition of the biomass is different, i.e., biomass contains a higher proportion of volatile matter and a smaller proportion of fixed carbon than coal. Biomasses contain 70-80% volatile matter while most of the volatile matter contents of coals studied in this laboratory did not exceed 45%, see Table 1 and Table A2 in Appendix 2. The aforementioned structural and chemical composition disparities resulted in the following combustion behavior differences between biomass studied herein and coal reported in Refs [32, 34, 48]:

(i) Pyrometric combustion intensities

The radiation intensity signals captured by the pyrometer during the combustion of biomass particles were weaker than those captured during combustion of coal particles under identical experimental conditions [48], especially during the phase of volatiles combustion. Moreover, the variability of the pyrometric signals of biomass particles was higher than those of coal, as there were more particle-to-particle size variations and shape irregularities in the biomass samples.

(ii) Volatile particle envelope flame combustion

The compounds released from biomass in the form of volatiles are different than those from coal. The cellulose and hemicellulose components of biomass decompose to small molecules in the form of volatile gases, tars and pyrolytic water [54]. These volatiles are

generally lighter than those formed from coal [23]. The volatile flames of biomasses were observed to be typically transparent, and nearly non-sooty, similar to those of low rank coals [32], whereas those of the bituminous coals were sooty. The percentage of bonded oxygen in biomasses is much higher than that of coals (Table 1 and Table A2). Therefore, the volatiles contain high quantities of CO and CO_2 as well as hydrogen and light hydrocarbons [24, 50, 51]. They also contain smaller amounts of tars and other condensables than the volatiles of coal particles. To the contrary, bituminous coal volatiles contain mostly heavy hydrocarbons, tars, condensables and light hydrocarbons [53]. In previous studies [31, 32, 33, 48], bituminous coal particles released a high amount of volatiles, with long soot-containing contrails forming in the wake of each settling particle whereas lignite coal particles released light hydrocarbons and CO, resulting in occasional, faint and brief volatile flames with a large extent of char fragmentation. Anthracite coals released very small amount of volatiles and did not establish an envelope flames. Biomass particles burned with distinctive volatiles flames without contrails. Unlike the combustion behavior of coals, which differs widely with rank, type and seam, the combustion behavior of biomasses from the four different sources of this study appears to be more unified. The ignition of biomass volatiles started earlier (shorter ignition delays) and their ensuing combustion occurred in envelope flames that were spherical and peripherally-uniform, even in the cases of elongated or otherwise irregularly-shaped particles. Furthermore, as biomass has a lower apparent density than coal (representative values for which have been reported as 1.32 g cm^{-3} for bituminous, 1.30 g cm^{-3} for subbituminous and 1.29 g cm^{-3} for lignite [56], whereas for biomasses is typically in the range of 0.4 - 0.5 g cm^{-3} [57], the burning biomass particles were very buoyant and settled very slowly in the furnace. The

observed volatile flame burnout times (Fig. 8) of the biomasses were generally much lengthier than those of the coal flames; for instance, they were lengthier than those of bituminous coal particles of comparable nominal size by a factor of eight [30, 32], which is much higher than the ratio of their volatile contents. This is likely due to the fact that because of their elongated shapes and, thus, their higher aspect ratios, biomass particles tend to be overall bigger than coal of the same size cut.

(iii) Char combustion

Whereas coal chars typically exhibited a rather uniform temperature profile during their combustion before experiencing a slow decrease towards burnout [30, 31, 32, 48], the temperature profile of biomass chars increased throughout their combustion history. Examples of biomass (bagasse) char and coal (bituminous) particle temperature-time profiles are illustrated in Figure 9 (the temperature of the volatile envelope flames of the biomass particles is not included in this plot, as it is currently under investigation). In general, biomass chars burned at a somewhat higher average temperature than bituminous char particles (by 50-100 K), as can be attested by comparing the results shown in Fig.8 and those in Refs. [30, 31, 32, 48]. Biomass char particles burned with lower average temperatures (by 100-200 K) than lignite char particles in similar gas environments. Moreover, the biomass char burnout times were much briefer than the coal particle chars burnout times due to lower fixed carbon content of the biomass. Biomass chars have higher reactivity than coal chars, as reported by Matsumoto et al. [58] and Ollero et al. [59]. Matsumoto et al. [58] showed that a woody biomass char had five times higher reactivity than a sub-bituminous coal char at high heating rates encountered in an entrained flow reactor and gas temperatures in the range of 1200-

1450 K. The higher reactivity of biomass char was partly attributed to faster char gasification reactions, such as C(s) + CO_2 => 2CO. This was also related to the higher concentration of alkali metals, which act as a catalyst and to the higher oxygen to carbon ratio in biomass char [58, 59].

4. Conclusions

Biomass particles were burned in a laboratory-scale drop-tube furnace at 1400 K in air and in different oxy-fuel atmospheres, simulated by dry O_2/CO_2 gases. Experiments were performed under quiescent gas conditions. Striking differences were observed between the combustion behavior of the biomass particles burned herein and those of coal particles of all ranks investigated in previous studies in this laboratory. The biomass particles released large amounts of volatiles that burned in the form of spherical envelope flames. Ensuing biomass char combustion produced stronger pyrometric signals than the combustion of the volatile matter. Increasing the oxygen mole fraction in CO_2 reduced the luminosity of the flames. The combustion intensity of the biomass was stronger in air (21% O_2-79% N_2) than in an oxy-fuel atmosphere with the same oxygen mole fraction (21% O_2-79% CO_2). Increasing the oxygen mole fraction in the CO_2 background gas enhanced the combustion intensity of biomass. It decreased the burnout times of volatiles and of the char residues, whereas it increased the temperature of the burning char particles. Similar trends were observed for all tested biomass samples from disparate sources, including the raw and torrefied pine sawdust. Thus, unlike the combustion behavior of coals, which differs widely with rank, type and seam, the combustion behavior of biomasses from the four different sources of this study appears more unified. Olive residue chars (OR) burned at lower temperatures than

the other biomass fuels, whereas bagasse chars (SCB) burned at higher temperatures than the other biomass fuels. The volatile flames of biomass particles are less sooty than those of bituminous coal particles.

Acknowledgments

The authors acknowledge financial assistance from the US-NSF award CBET-0755431. J. Riaza acknowledges funding from the Government of the Principado de Asturias (Severo Ochoa program). M.V. Gil and L. Álvarez acknowledge funding from the CSIC JAE programme co-financed by the European Social Fund.

References

[1] Kazanc F, Khatami R, Crnkovic PM, Levendis YA. Emissions of NO_x and SO_2 from coals of various ranks, bagasse, and coal-bagasse blends burning in O_2/N_2 and O_2/CO_2 environments. Energy and Fuels 2011;25(7):2850-61.

[2] Riaza J, Gil MV, Álvarez L, Pevida C, Pis JJ, Rubiera F. Oxy-fuel combustion of coal and biomass blends. Energy 2012;41(1):429-35.

[3] Tillman DA. Biomass cofiring: the technology, the experience, the combustion consequences. Biomass and Bioenergy 2000;19(6):365-84.

[4] Baxter L. Biomass-coal co-combustion: opportunity for affordable renewable energy. Fuel 2005;84(10):1295-302.

[5] Smart JP, Patel R, Riley GS. Oxy-fuel combustion of coal and biomass, the effect on radiative and convective heat transfer and burnout. Combustion and Flame, 2010;157(12):2230-40.

[6] Álvarez L, Riaza J, Gil MV, Pevida C, Pis JJ, Rubiera F. NO emissions in oxy-coal combustion with the addition of steam in an entrained flow reactor. Greenhouse Gases: Science and Technology 2011;1(2):180-90.

[7] Simpson AP, Simon AJ. Second law comparison of oxy-fuel combustion and post-combustion carbon dioxide separation. Energy Conversion and Management 2007;48(11):3034–45.

[8] Haykiri-Acma H, Turan AZ, Yaman S, Kucukbayrak S. Controlling the excess heat from oxy-combustion of coal by blending with biomass. Fuel Processing Technology 2010;91(11):1569-75.

[9] Saidur R, Abdelaziz EA, Demirbas A, Hossain MS, Mekhilef S. A review on biomass as a fuel for boilers. Renewable and Sustainable Energy Reviews 2011;15(5):2262-89.

[10] Yang H, Yan R, Chen H, Lee DH, Zheng C. Characteristics of hemicellulose, cellulose and lignin pyrolysis. Fuel 2007;86 (12-13):1781-8.

[11] Cui H, Grace JR. Spouting of biomass particles: A review. Bioresource Technology 2008;99(10):4008-20.
[12] Ratte J, Fardet E, Mateos D, Héry JS. Mathematical modelling of a continuous biomass torrefaction reactor: TORSPYD column. Biomass and Bioenergy 2011;35(8):3481-95.
[13] Rousset P, Aguiar C, Labbé N, Commandré J-M. Enhancing the combustible properties of bamboo by torrefaction. Bioresource Technology 2011;102(17):8225-31.
[14] Fisher EM, Dupont C, Darvell LI, Commandré JM, Saddawi A, Jones JM. Combustion and gasification characteristics of chars from raw and torrefied biomass. Bioresource Technology 2012;119:157-65.
[15] Arias B, Pevida C, Fermoso J, Plaza MG, Rubiera F, Pis JJ. Influence of torrefaction on the grindability and reactivity of woody biomass. Fuel Processing Technology 2008;89(2):169-75.
[16] van der Stelt MJC, Gerhauser H, Kiel JHA, Ptasinski KJ. Biomass upgrading by torrefaction for the production of biofuels: A review. Biomass and Bioenergy 2011;35(9):3748-62.
[17] Verhoeff F, Adell A, Boersma AR, Pels JR, Lensselink J, Kiel JHA. TorTech: Torrefaction as key technology for the production of (solid) fuels from biomass and residue, ECN report, ECN-E--11-039, 2011.22
[18] Demirbas A. Combustion characteristics of different biomass fuels. Progress in Energy and Combustion Science 2004;30(2):219-30.
[19] Williams A, Pourkashanian M, Jones JM. Combustion of pulverised coal and biomass. Progress in Energy and Combustion Science 2001;27(6):587-610.
[20] van Loo S, Koppenjan J, The handbook of biomass combustion and co-firing. London: Earthscan; 2008.
[21] Bridgwater AV. Review of fast pyrolysis of biomass and product upgrading. Biomass and Bioenergy 2012;38:68-94.
[22] White J, Catallo W, Legendre B. Biomass pyrolysis kinetics: A comparative critical review with relevant agricultural residue case studies. Journal of Analytical and Applied Pyrolysis 2011;91(1):1.
[23] Babu BV, Chaurasia AS. Heat transfer and kinetics in the pyrolysis of shrinking biomass particle. Chemical Engineering Science 2004;59(10):1999-2012.
[24] Neves D, Thunman H, Matos A, Tarelho L, Gómez-Barea A. Characterization and prediction of biomass pyrolysis products. Progress in Energy and Combustion Science 2011;37(5):611-30.
[25] Timothy LD, Sarofim AF, Beer JM. Characteristics of single particle coal combustion. Proceedings of the Combustion Institute 1982;19(1):1123-30.
[26] Levendis YA, Flagan RC, Gavalas GR. Oxidation kinetics of monodisperse spherical carbonaceous particles of variable properties. Combustion and Flame 1989;76(3-4):221-41.
[27] Loewenberg M, Levendis YA. Combustion behavior and kinetics of synthetic and coal-derived chars: Comparison of theory and experiment. Combustion and Flame 1991;84(1-2):47-65.
[28] Levendis YA, Estrada KR, Hoyt CH. Development of multicolor pyrometers to monitor the transient response of burning carbonaceous particles. Review of Scientific Instruments 1992;63(7):3608-22.

[29] Atal A, Levendis YA. Comparison of the combustion behaviour of pulverized residue tyres and coal. Fuel 1995;74(11):1570-81.
[30] Bejarano PA, Levendis YA. Single-coal-particle combustion in O_2/N_2 and O_2/CO_2 environments. Combustion and Flame 2008;153(1-2):270-87.
[31] Levendis YA, Joshi K, Khatami R, Sarofim AF. Combustion behavior in air of single particles from three different coal ranks and from sugarcane bagasse. Combustion and Flame 2011;158(3):452-65.
[32] Khatami R, Stivers C, Joshi K, Levendis YA, Sarofim AF. Combustion behavior of single particles from three different coal ranks and from sugar cane bagasse in O_2/N_2 and O_2/CO_2 atmospheres. Combustion and Flame 2012;159(3):1253-71.
[33] Khatami R, Stivers C, Levendis YA. Ignition characteristics of single coal particles from three different ranks in O_2/N_2 and O_2/CO_2 atmospheres. Combustion and Flame, 2012;159(12):3554-68.
[34] Wornat MJ, Hurt RH, Davis KA, Yang NYC. Single-particle combustion of two biomass chars. Symposium (International) on Combustion 1996;26(2):3075-83.
[35] Austin PJ, Kauffman CW, Sichel M. Ignition and volatile combustion of cellulosic dust particles. Combustion Science and Technology 1996;112(1):187-98.
[36] Meesri C, Moghtaderi B. Experimental and numerical analysis of sawdust-char combustion reactivity in a drop tube reactor. Combustion Science and Technology 2003;175(4):793-823.
[37] Arias B, Pevida C, Rubiera F, Pis JJ. Effect of biomass blending on coal ignition and burnout during oxy-fuel combustion. Fuel 2008;87(12):2753-59.
[38] Borrego AG, Garavaglia L, Kalkreuth WD. Characteristics of high heating rate biomass chars prepared under N_2 and CO_2 atmospheres. International Journal of Coal Geology 2009;77(3-4):409-15.
[39] Yang YB, Sharifi VN, Swithenbank J, Ma L, Darvell LI, Jones JM et al. Combustion of a single particle of biomass, Energy and Fuels 2008;22(1):306-16.
[40] Lu H, Robert W, Peirce G, Ripa B, Baxter LL. Comprehensive study of biomass particle combustion. Energy and Fuels 2008;22(4):2826-39.
[41] Thunman H, Leckner B, Niklasson F, Johnsson F. combustion of wood particles - a particle model for eulerian calculations. Combustion and Flame 2002;129:30-46.
[42] Karlström O, Brink A, Hupa M. Time dependent production of NO from combustion of large biomass char particles. Fuel 2013;103:524-32.
[43] Toftegaard MB, Brix J, Jensen PA, Glarborg P, Jensen AD. Oxy-Fuel combustion of solid fuels. Progress in Energy and Combustion Science 2010;36(5):581-625.
[44] Khatami R, Levendis YA. On the deduction of single coal particle combustion temperature from three-color optical pyrometry. Combustion and Flame 2011;158(9):1822-36.
[45] Grotkjaer T, Dam-Johansen K, Jensen AD, Glarborg P. An experimental study of biomass ignition. Fuel 2003;82(7):825-33.
[46] Shaddix C, Hecht E, Geier M, Molina A, Haynes B. Effect of gasification reactions on oxy-fuel combustion of pulverized coal char. Proceedings of the 35th Conference of Coal Combustion and Fuel Systems, Clearwater, Florida , July 1-5, 2010.

[47] Maffei T, Khatami R, Pierucci S, Faravelli T, Ranzi E, Levendis Y. Experimental and modeling study of single coal particle combustion in O_2/N_2 and oxy-fuel (O_2/CO_2) atmospheres. Combustion and Flame 2013;160:2559-2572.
[48] Riaza J, Khatami R, Levendis Y, Álvarez L, Gil MV, Pevida C, Rubiera F, Pis JJ. Single particle ignition and combustion of anthracite, semi-anthracite and bituminous coals in air and simulated oxy-fuel conditions. Combustion and Flame 2014;161:1096-1108.
[49] Sun S, Tian H, Zhao Y, Sun R, Zhou H. Experimental and numerical study of biomass flash pyrolysis in an entrained flow reactor. Bioresource Technology 2010;101(10):3678-84.
[50] Alves J, Zhuo C, Levendis Y, Tenorio J. Catalytic conversion of wastes from the bio-ethanol production into carbon nanomaterials. Applied Catalysis B. Environmental 2011;106:433-444.
[51] Davies A, Soheilian R, Zhuo C, Levendis Y. Pyrolytic conversion of biomass residues to gaseous fuels for electricity generation", Journal of Energy Resources Technology. Transactions of ASME, 2013;136(2):021101-07.
[52] Bragato M, Joshi K, Carlson JB, Tenório JAS, Levendis YA. Combustion of coal, bagasse and blends thereof: Part I: Emissions from batch combustion of fixed beds of fuels. Fuel 2012;96:43-50.
[53] Bragato M, Joshi K, Carlson JB, Tenório JAS, Levendis YA. Combustion of coal, bagasse and blends thereof: Part II: Speciation of PAH emissions. Fuel 2012;96:51-58.
[54] Zhang H, Xiao R, Wang D, He G, Shao S, Zhang J et al. Biomass fast pyrolysis in a fluidized bed reactor under N_2, CO_2, CO, CH_4 and H_2 atmospheres. Bioresource Technology 2010;102(5):4258-64.
[55] McLean W, Hardesty D, Pohl J, Direct observations of devolatilizing pulverized coal particles in a combustion environment. Proceedings of the Combustion Institute. 1981;18(1):1239-1248.
[56] Wood G, Kehn T, Carter M, Culbertson W. Coal resource classification system of the U.S. Geological Survey. U.S. Geological Survey circular 1983;891.
[57] Basu P. Biomass gasification, pyrolysis and torrefaction: practical design and theory. 4th ed. London: Elsevier Inc., 2013.
[58] Matsumoto K, Takeno K, Ichinose T, Ogi T, Nakanishi M. Gasification reaction kinetics on biomass char obtained as a by-product of gasification in an entrained-flow gasifier with steam and oxygen at 900-1000C. Fuel 2009;88(3):519-27.
[59] Ollero P, Serrera A, Arjona R, Alcantarilla S. The CO_2 gasification kinetics of olive residue. Biomass and Bioenergy 2003;24(2):151-61.

Appendix 1

Calculation of the oxygen mole fraction at the biomass char particle surface and of the diffusion-limited burnout time.

Based on a derivation by Levendis et al.[26], the average oxygen mole fraction on the char particle surface can be estimated by the following formula:

$$y_{O_2 s} = (4/3 + y_{O_2 \infty})\, e^{-\left(\frac{a_0^2 R T_m \rho_c}{56 P_{tot} D t_{B,obs}}\right)} - 4/3 \qquad (A.1)$$

In this relation, y_{O2} is assumed to be an average value. a_i, ρ_c, T_m, D, t_B, R and P_{tot} are initial burning particle radius, initial particle density, film temperature between the char particle and flow, bulk diffusion coefficient of O_2 in the diluents gas, observed particle burnout time, gas universal constant and total pressure of the system, respectively.

If $y_{O_2 s}$ is zero or close to zero, the combustion takes place at diffusion limited conditions (Regime III), whereas if $y_{O_2 s}$ is close to $y_{O_2 \infty}$, the combustion happens at kinetically limited condition (Regime I). Any $y_{O_2 s}$ in-between the above values results in kinetic-diffusion limited condition (Regime II).

The time t_B required for combustion under diffusion control (Regime III) becomes [26]:

$$t_B = \frac{\rho_c (a_i^2 - a_f^2)}{56} \frac{RT_m}{D} \frac{1}{\ln(1 + \frac{3}{4} y_{O_2 \infty})} \qquad (A.2)$$

In Eq. A.2, a_f is the final particle radius after extinction, which herein is estimated based on the ash content in the parent biomass composition.

For instance, for sugarcane bagasse burning in air with the observed parameters of this study a_{0i}=15(μm), a_f=2.5 (μm), ρ_c=0.2 (g/cm^3), T_m=1600 K, P_{tot}=1 (atm), $D_{O2\text{-}N2}$=3.49 (cm^2/s), $t_{B\text{-}obs}$=18 (ms), R=82 (atm.cm^3/mol.K), oxygen mole fraction on the particle

surface from A.1, $y_{O_2 s}$, was calculated to be 0.08 and the diffusion limited burnout time from A.2, t_B, was calculated to be 10 (ms). On the other hand, for sugarcane bagasse burning in 21%O_2-79%CO_2, T_m=1500 K, $D_{O2\text{-}CO2}$=2.73(cm^2/s), $t_{B\text{-}obs}$=23 (ms) and the rest of parameters are similar to those of combustio in air. In this case, oxygen mole fraction on the particle surface from A.1, $y_{O_2 s}$, was 0.09 and the diffusion limited burnout time from A.2, t_B, was 12 (ms). Therefore, under the experimental conditions of this study, combustion of bagasse in either air or oxy-fuel condition (21%O_2-79%CO_2) took place in Regime II which is a combination of kinetic and diffusion limited cases. From Eq. A.2 for diffusion limited case, the burnout time is inversely proportional to the mass diffusivity of oxygen in the diluents gas and this seems to be the case in the current work, because:

$$\frac{t_{B-obs-Air}}{t_{B-obs-21\%O_2/79\%CO_2}} = \frac{18}{23} = 0.78 \approx \frac{D_{O_2-CO_2}}{D_{O_2-N_2}} = \frac{2.73}{3.49} = 0.77$$

The resulted observed burnout times and calculated diffusion limited burnout times versus oxygen concentration for sugarcane bagasse in different oxy-fuel condition is shown in Fig. A.1.

Appendix 2

Characterization of coals used for comparison with the biomasses [32, 48].

Table 1: Biomass type, origin and chemical composition

Sample	Origin	Proximate Analysis (wt%, db)			Ultimate Analysis (wt%, daf)					HHV (MJ/kg)
		Ash	V.M.	F.C.*	C	H	N	S	O*	
OR	Olive residue	7.6	71.9	20.5	54.3	6.6	1.9	0.2	37.0	19.9
SCB	Sugarcane bagasse	4.2	87.8	8.0	46.3	5.9	0.2	0.1	47.5	16.3
PI	Pine sawdust	3.8	79.8	16.4	45.9	6.1	0.7	0	47.3	18.9
TOPI	Torrefied pine sawdust	4.2	75.5	20.3	51.2	5.7	0.9	0	42.2	20.2

* determined by difference

Table A2: Coals used for purposes of comparison with biomasses: rank,/type and chemical composition [34, 53]

Sample	Rank/Type	Proximate Analysis (wt%, db)			Ultimate Analysis (wt%, daf)					HHV (MJ/kg)
		Ash	V.M.	F.C.*	C	H	N	S	O*	
AC [53]	Anthracite	14.2	3.6	82.2	94.7	1.6	1.0	0.7	2.0	29.2
PSOC-1451[34]	Bituminous	13.3	33.6	50.6	71.9	4.7	1.4	1.4	6.9	31.5
DECS-26 [34]	Sub-bituminous	5.6	33.1	35.1	69.8	5.7	0.9	0.4	15.6	28.2
PSOC-1443 [34]	Lignite	15.3	44.2	12.0	56.8	4.1	1.1	0.7	15.8	23.0

* determined by difference

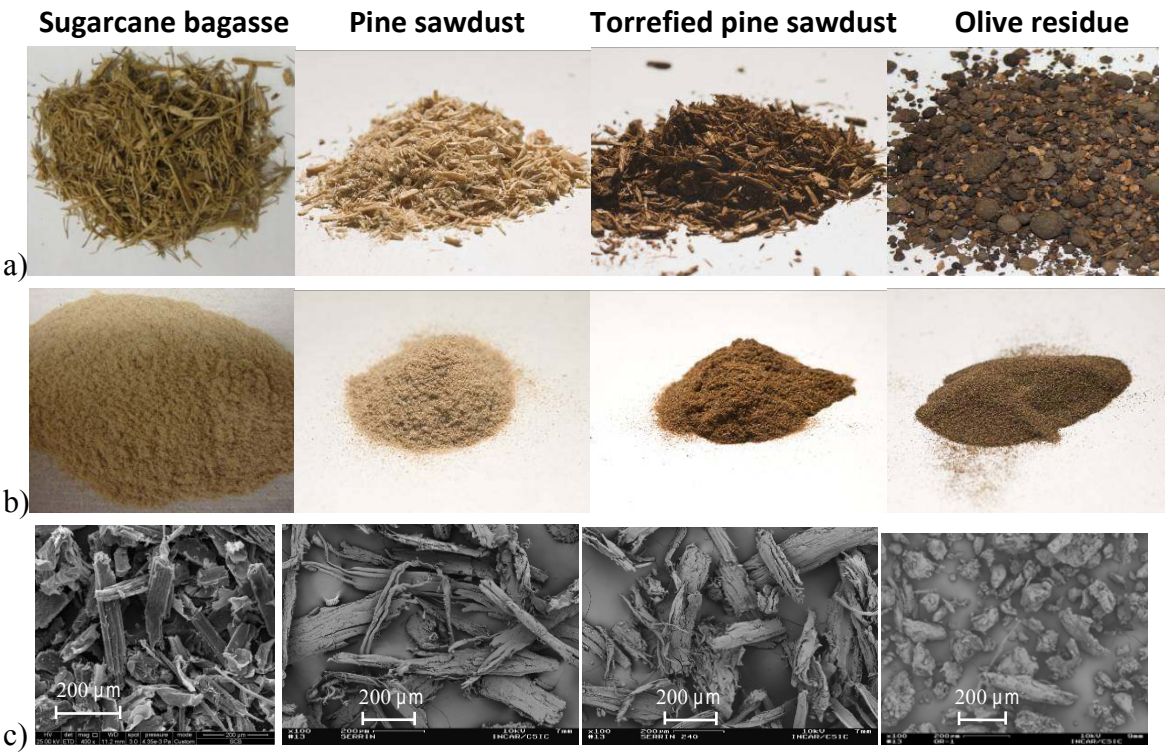

Figure 1. Physical appearance of the biomasses residue; (a) original biomasses, as received, (b) ground and sieved, (c) SEM micrographs detailing individual particles.

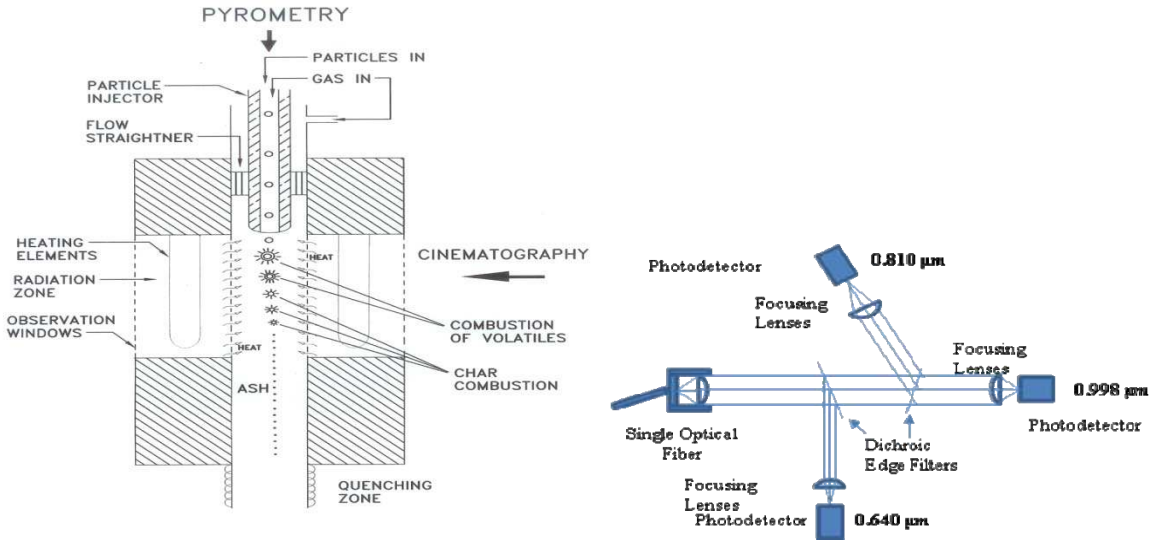

(a) (b)

(c)

Figure 2. Schematic of the experimental setup and diagnostic facilities. (a) Laminar-flow, electrically-heated drop-tube furnace (DTF), (b) Three-color optical pyrometer, (c) High speed camera (NAC) fitted with a long-range microscope lens (Infinity K2).

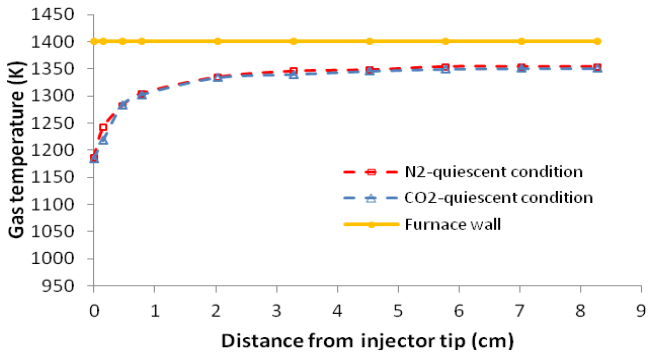

Figure 3. The centerline furnace gas temperature under quiescent conditions (no gas flow)[47].

a) Sugar cane bagasse

Bagasse – AIR

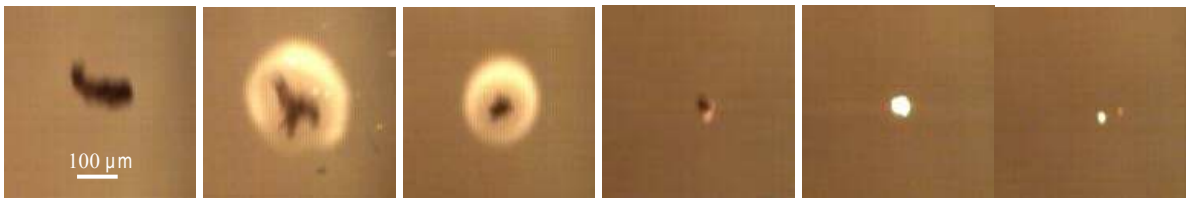

0 4 17 30 49 58

Bagasse - Oxy 21%

0 9 14 34 39 48

Bagasse - Oxy 30%

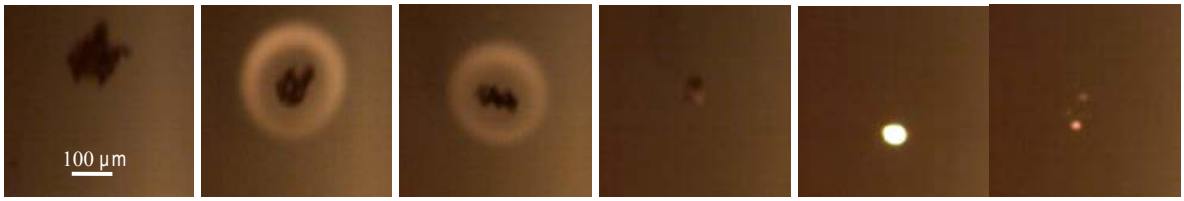

0 8 12 28 36 43

Bagasse - Oxy 35%

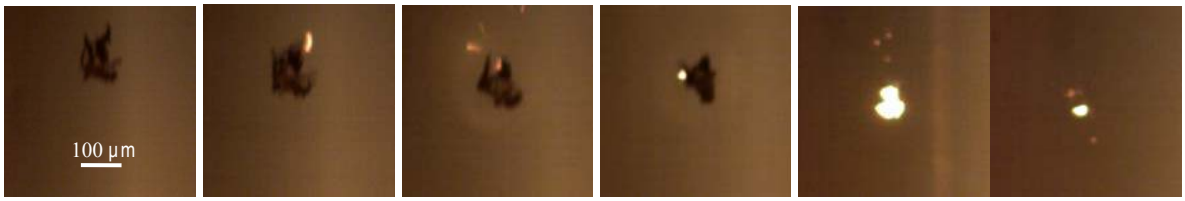

0 2 6 10 30 46

Bagasse - Oxy 50%

0 4 19 24 26 27

b) Olive residue

OR - Air

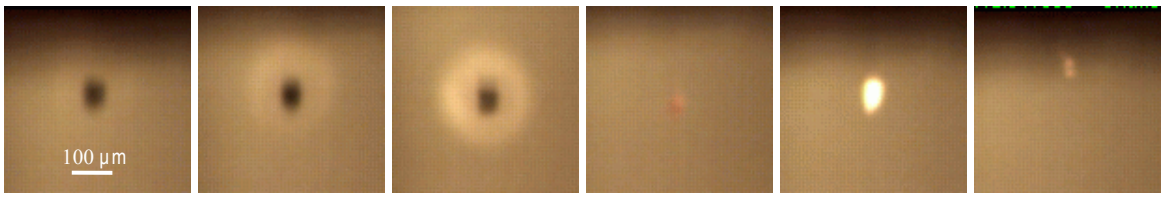

OR - Oxy 21%

OR - Oxy 30%

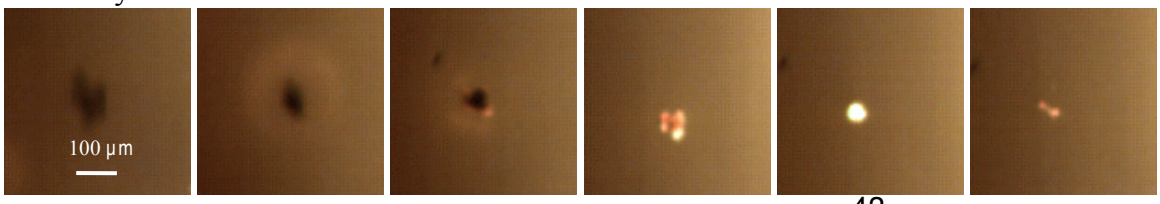

OR - Oxy 35%

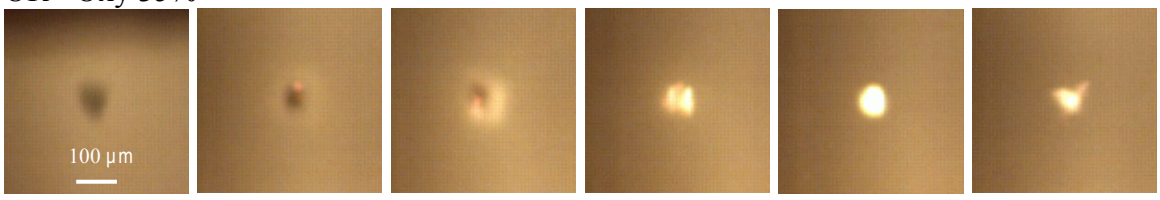

OR - Oxy 50%

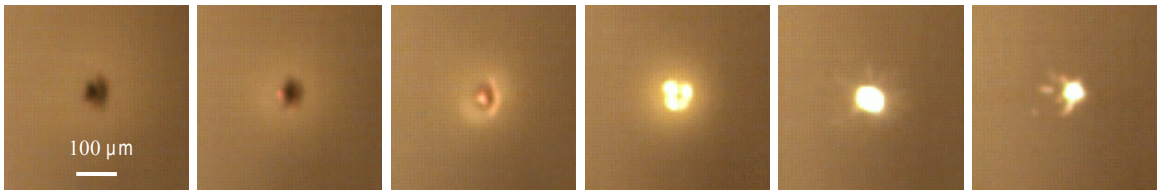

c) Pine sawdust

PI - Air

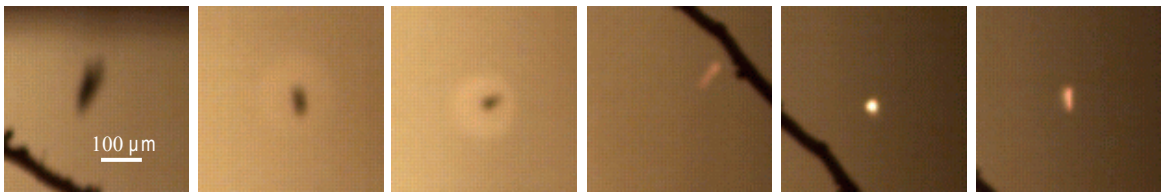

0 8 13 19 28 42

PI - Oxy 21%

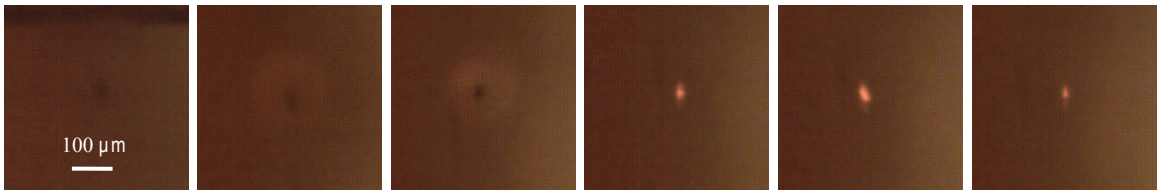

0 4 9 18 21 26

PI - Oxy 30%

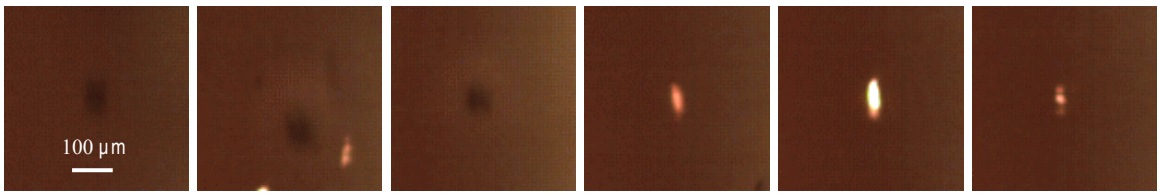

0 2 8 23 36 42

PI - Oxy 35%

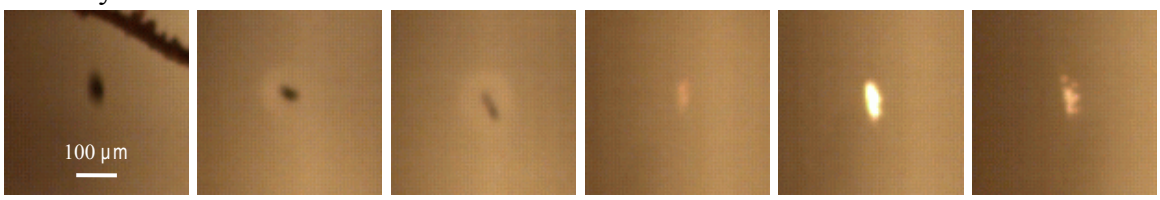

0 8 10 13 15 26

PI - Oxy 50%

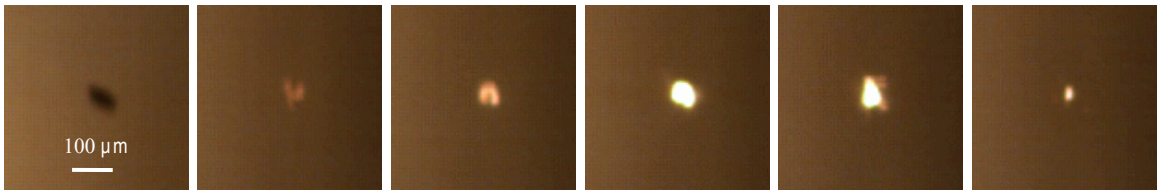

0 1 2 4 6 8

d) Torrefied pine sawdust

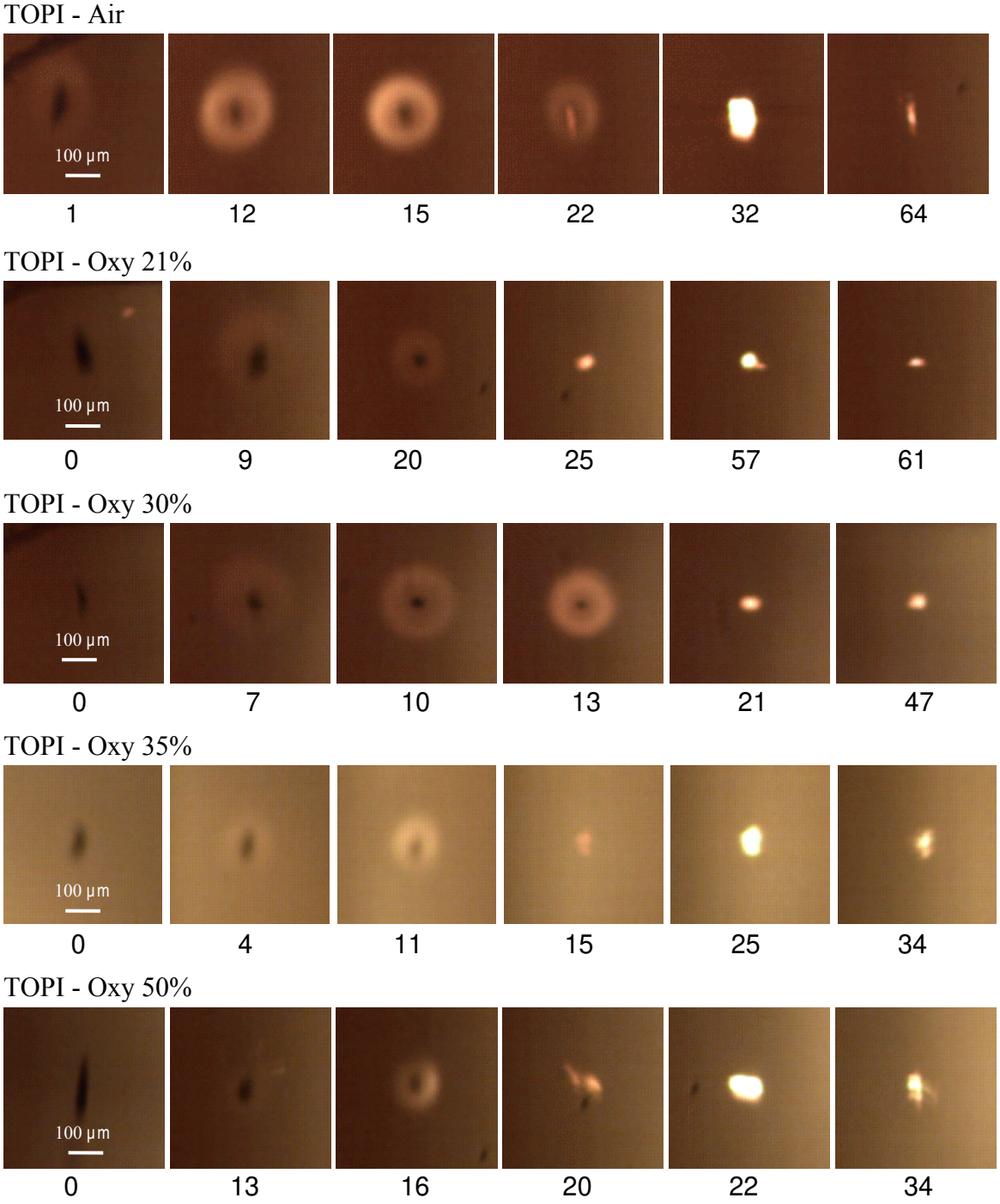

Figure 4. High-speed, high magnification cinematography images of single particles of biomass residuees in different atmospheres. Displayed numbers under each image represent frame times of combustion in milliseconds. Biomass samples are: a) sugarcane bagasse (SCB), b) olive residue (OR), c) pine sawdust (PI), and d) torrefied pine sawdust (TOPI).

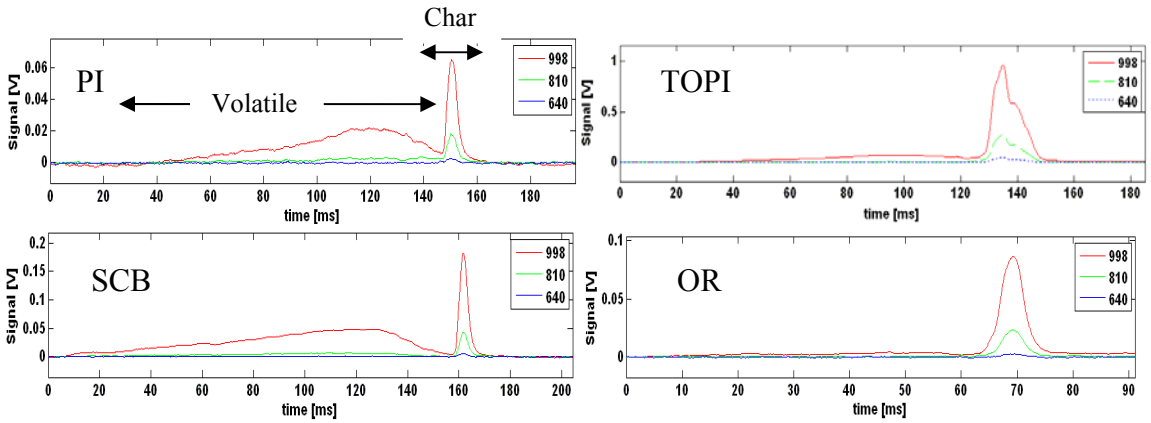

Figure 5. Three-color pyrometry – generated signals from single particles of biomass residues burning in air. Biomass samples are: pine sawdust (PI), torrefied pine sawdust (TOPI), sugarcane bagasse (SCB), and olive residue (OR).

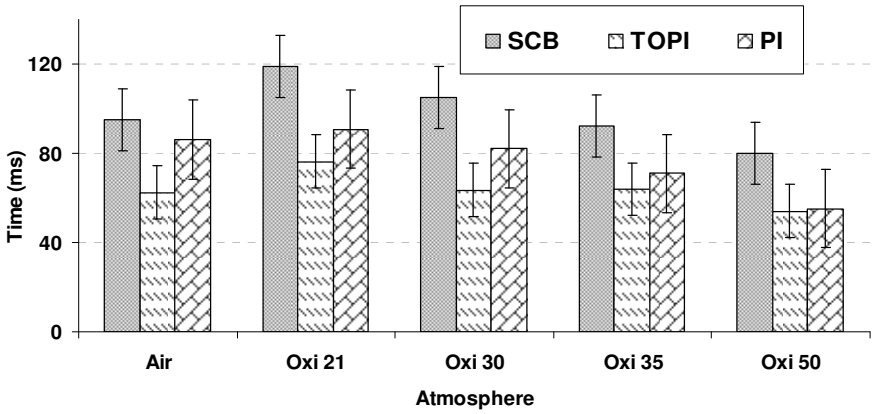

Figure 6. Average burnout times for the volatiles of three of the biomass fuels of this work (sugarcane bagasse (SCB), pine sawdust (PI) and torrefied pine sawdust (TOPI)) burning in air and in different oxy-fuel atmospheres.

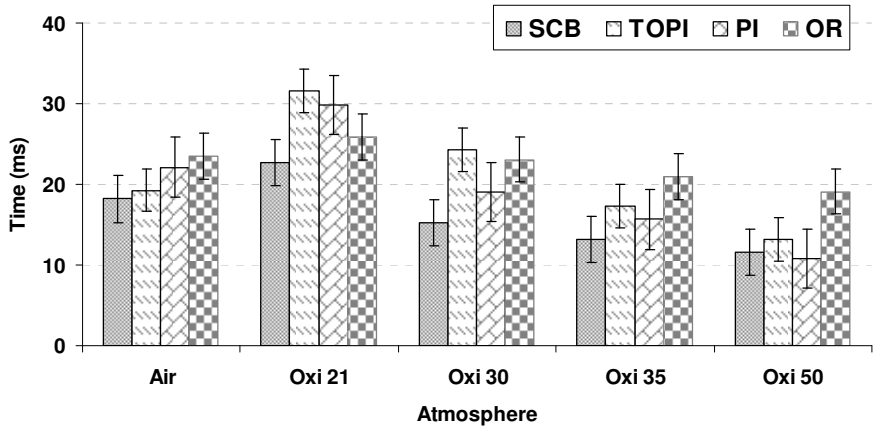

Figure 7. Average burnout times for the chars of all the biomass fuels of this work (sugarcane bagasse (SCB), pine sawdust (PI), torrefied pine sawdust (TOPI and olive residue (OR)) burning in air and in different oxy-fuel atmospheres.

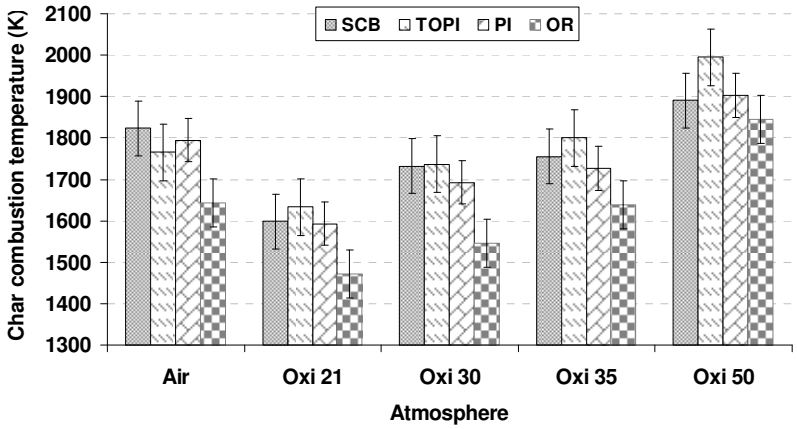

Figure 8. Average deduced temperatures for the burning chars of all the biomass fuels of this work (pinesawdust (PI), torrefied pine sawdust (TOPI), sugarcane bagasse (SCB),and olive residue (OR)) burning in air and in different oxy-fuel atmospheres.

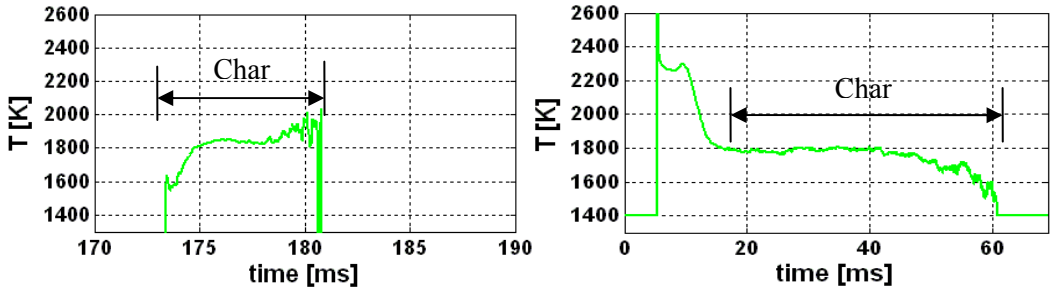

Figure 9. Deduced temperature-time profiles of single particles of biomass (sugar cane bagasse) and coal (bituminous) burning in air. The original particle sizes are 75-90µm for both fuels.The biomass char size is 25-30µm. The temperature of biomass char increases during the combustion history of the particle whereas that of the coal char remains mostly constant.

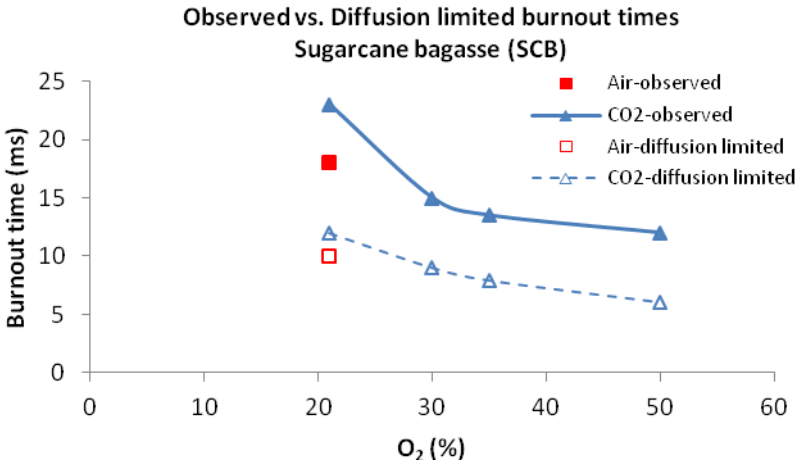

Figure A.1. Comparison of experimentally-observed and calculated diffusion-limited burnout times of sugarcane bagasse char particles, plotted against bulk oxygen mole fraction.